KJNMT. 2023 November, 27(2)83-93
https://doi.org/10.12972/kjnmt.20230014

pISSN 1229-9901
eISSN 2982-8406

Review article

Synthesis of Novel ^{18}F-Labeled-Nitroimidazole-Based Imaging Agents for Hypoxia: Recent Advances

Anh Thu Nguyen[1,2] and Hee-Kwon Kim[1,2]

[1]Deparment of Nuclear Medicine, Jeonbuk National University, Jeonju, Korea

[2]Deparment of Medical Science, Jeonbuk National University, Jeonju, Korea

*Corresponding Author : Hee-Kwon Kim. Department of Nuclear Medicine, Jeonbuk National University, 20, Geonji-ro, Deokjin-gu, Jeonju-si, Jeollabuk-do, 54907, Rep. of Korea. Tel :+82-63-250-2768, E-mail : hkkim717@jbnu.ac.kr

ABSTRACT

Hypoxia indicates the condition of low oxygen levels in tissues. In oncology, hypoxia can induce cancer progression and metastasis, as well as cause resistance to cancer therapies. The detection of hypoxia by using molecular imaging, particularly, positron emission tomography (PET) has been extensively studied due to many advantages. Nitroimidazoles, the moieties that can be trapped in hypoxic tissues due to selective reduction, have been used to design and synthesize of hypoxia-targeting radiopharmaceuticals. This review provides a summary of synthetic routes towards ^{18}F-labeled-nitroimidazole radiotracers for PET imaging of hypoxia.

Key words: Hypoxia, Radiotracers, PET, Nitroimidazole, Tumor

Introduction

Molecular imaging is the noninvasive visualization, characterization and measurement of biological activities occurring at molecular or cell level [1]. Over the past few decades, there has been a growing trend towards the applications of molecular imaging in various fields [2]. Positron emission tomography (PET) is a molecular imaging technique detecting gamma-ray radiation released by positron-emitting radioisotopes such as fluorine-18, carbon-11, oxygen-15, and nitrogen-13 of radiolabeled compounds, namely radiopharmaceuticals [3]. PET has been widely used in preclinical and clinical studies to detect and quantify biological processes of a variety of diseases due to its advantages including deep penetration into body tissues and high sensitivity [4,5]. PET imaging has demonstrated an essential role in the diagnosis and treatment of various types of cancer within the field of oncology [6]. In the application of PET imaging in cancer treatment, developing radiopharmaceuticals with high selectivity for tumor and probable pharmacokinetics is vital to obtain high-resolution PET images and valuable information on the tumor progression, as well as to monitor responses to cancer therapies [7,8].

Hypoxia is defined as the condition of an inadequate oxygen supply in tissues which changes the biological functions [9]. In solid tumors, hypoxia is a characteristic found in most solid tumors because the proliferation of tumor cells exceeds the oxygen supply by blood vessels. Moreover, tumor hypoxia can increase the risk of metastasis, angiogenesis and tumor survival, thereby affect the response to cancer therapies [10]. Radiolabeled nitroimidazole derivatives have been studied extensively in the field of tumor hypoxia as hypoxia-targeting agents due to the selectively bioreduction of nitroimidazole moiety under hypoxic conditions [11].

Received July 11, 2023 **Revised** July 30, 2023 **Accepted** August 01, 2023

Among the positron-emitting radioisotopes, fluorine-18 is used most widely for the production of radiolabeled compounds. Fluorine-18 has several favorable chemical and physical properties such as long and convenient half-life of 109.8 min, small size, and ability to form strong and stable C-F bond [12]. This review provides a recent synthesis of 18F-labeled PET radiotracers in the field of hypoxia tumors since 2015.

Development of ^{18}F-labeled radiotracers for hypoxia

1. ^{18}F-labeled carbohydrate-based radiotracers

1. Synthesis of β-6'-[^{18}F]FAZAL

^{18}F-labeled radiotracer β-6′-[^{18}F]FAZAL (1-(6′-deoxy-6′-[^{18}F]fluoro-β-D-allofuranosyl)-2-nitroimidazole, β-[^{18}F]6) was developed by Wanek et al. in 2016 [13]. The precursor β-5 was synthesized from 1,2:5,6-di-*O*-isopropylidene-α-D-allofuranose 1. Acetylation and elimination of the 5,6-*O*-isopropylidene group converted 1 to 5,6-diol 2. The selective monotosylation of 2 to prevent detosylation, followed by acetylation of the 5-OH group afforded compound 3. Removing the 1,2-isopropylidene group from 3 using trifluoroacetic acid (TFA) and then acetylating with Ac_2O gave a mixture of tetraacetates α- and β-4 (α:β = 3:1). The tetraacetate mixture was coupled with 2-nitroimidazole (2-NI) using a modified Vorbrüggen method [14] to afford nucleosides α- and β-5 with 5% and 44% yields, respectively. Radiofluorination of β-5 was achieved via nucleophilic substitution of the tosylate group of β-5 with ^{18}F in the presence of dried tetrabutylammonium [^{18}F]fluoride complex in DMSO at 115 °C, and then deprotection of the obtained ^{18}F-labeled intermediate by sodium hydroxide. β-[^{18}F]6 was prepared with 12 ± 8% decay-corrected radiochemical yield (RCY), and the specific activity was 218 ± 58 GBq/lmol (Fig. 1). In PET imaging using EMT6 tumor-bearing mice, β-[^{18}F]6 showed good selectivity for hypoxic breathing with higher tumor-to-muscle and tumor-to-blood ratios than under normoxic breathing protocol.

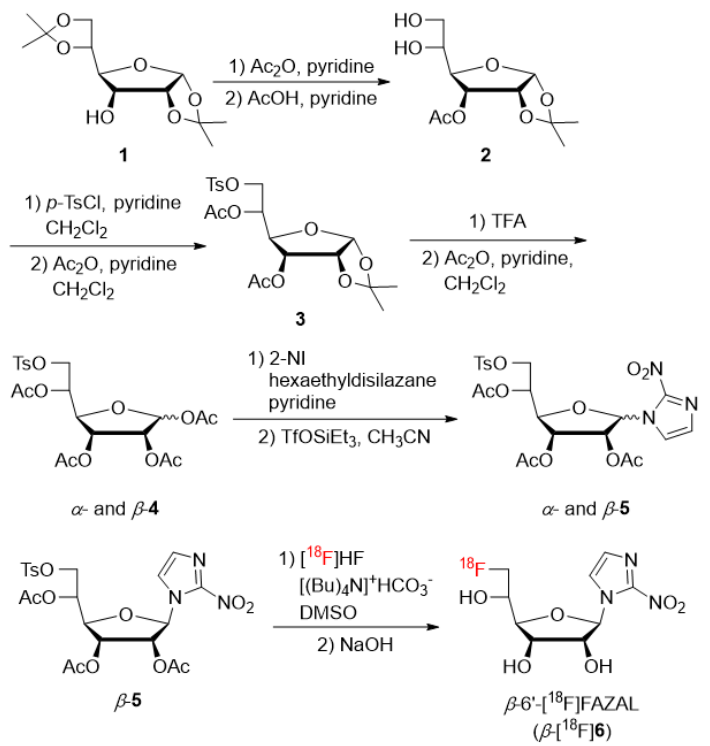

Fig. 1. Synthesis of radiolabeling nucleosides α- and β-5 and radiosynthesis of β-6'-[^{18}F]FAZAL (β-[^{18}F]6).

2. Synthesis of [^{18}F]FAZDR

Another ^{18}F-labeled carbohydrate derivative, [^{18}F]FAZDR ([^{18}F]fluoro-azomycin-2′-deoxy-β-D-ribofuranoside, [^{18}F]-β-11), was prepared by Schweifer et al. in 2016 [15]. The [^{18}F]FAZDR precursor was prepared from methyl 2-deoxy-D-ribofuranosides α- and β-7. Silylation of the primary OH group and acetylation of the secondary OH group of α- and β-7 gave methyl glycosides α- and β-8. Reactions of α- and β-8 with HCl/Et_2O produced the corresponding glycosyl chlorides which were then coupled with 2-nitroimidazole using the tetrabutylammonium salt of 2-nitroimidazole to afford compounds α-9 and β-9. Deprotection of α-9 and β-9 with KF/$PhCO_2H$, followed by tosylation with *p*-tosyl chloride in pyridine afforded the desired precursors α-10 and β-10. Isomer β-10 was chosen for radiolabeling because its structure was more similar to the nucleoside structure than α-10. Radiosynthesis of [^{18}F]FAZDR was performed by nucleophilic substitution of the tosyl group of precursor β-10 with ^{18}F. [^{18}F]FAZDR was prepared in 10.9 ± 2.4% RCY with >98% radiochemical purity and >50 GBq/μmol specific activity (Fig. 2). In vivo PET imaging experiments demonstrated the selective accumulation of [^{18}F]-β-10 under hypoxic conditions in CT26-tumor bearing BALB/c mice with a tumor-to-muscle ratio of 1.69 at 1 h post injection (p.i.).

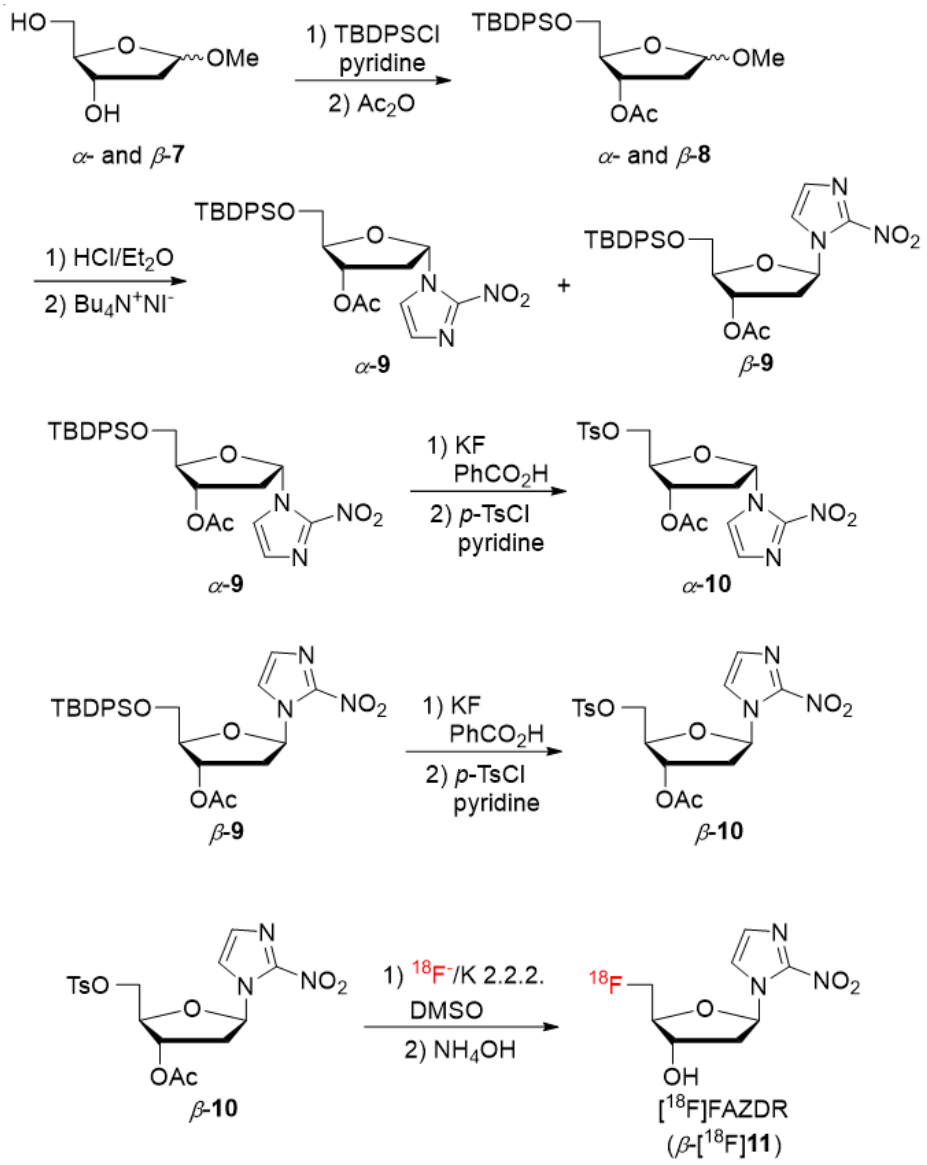

Fig. 2. Synthesis of the precursors α-9 and β-9 and radiosynthesis of [^{18}F]FAZDR ([^{18}F]-β-11).

3. Synthesis of α-[^{18}F]FAZDR

Four compounds β-FAZA, FAZA, α-FAZDR and β-FAZDR were synthesized and radiofluorinated with ^{18}F by Maier et al. in 2019 (Fig. 3) to study the effect of configuration of 2-nitroimidazole pharmacophore and sugar moieties on the detection of hypoxia in tumors [15,16]. The compound 1-(2-*O*-acetyl-β-D-arabinofuranosyl)-2-nitroimidazole (β-12) was selectively silylated using TBDMSCl and imidazole in pyridine, then acetylated with acetic anhydride to give compound β-13. Fluorination of β-13 with Deoxo-Fluor® generated compound β-14, which was then converted to β-FAZA (β-15) via the deprotection of acetyl groups with MeONa in MeOH [17]. Radiolabeling of α-16 via the nucleophilic substitution of the tosyl group with ^{18}F, followed by deprotection of the acetyl group with NH_4OH provided the target radiotracer (α-[^{18}F]FAZDR) with 15.9 ± 9.0% RCY, >50 GBq/μmol molar activity, and >98% radiochemical purity (Fig. 4). Both α- and β- [^{18}F]FAZDR demonstrated potential for hypoxia targeting with the high tumor-to-muscles ratios when tested in vivo.

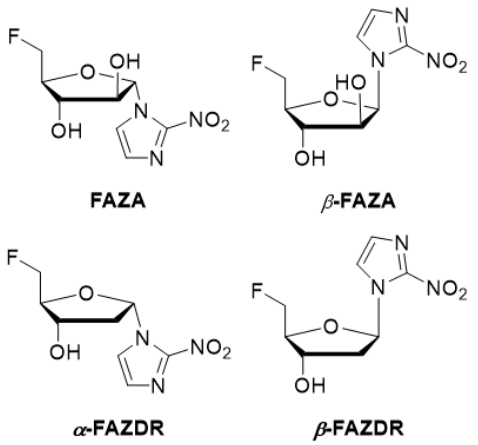

Fig. 3. Chemical structures of fluorinated C5-sugars containing 2-nitroimidazoles β-FAZA, FAZA, α-FAZDR and β-FAZDR.

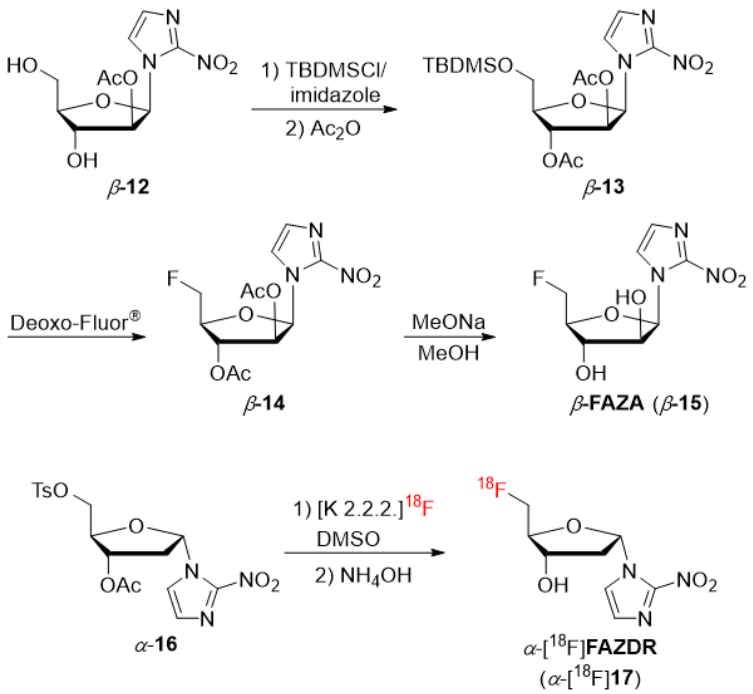

Fig. 4. Synthesis of β-FAZA from 1-(2-*O*-acetyl-β-D-arabinofuranosyl)-2-nitroimidazole (β-38) and radiosynthesis of α-[^{18}F] FAZDR.

4. Synthesis of [^{18}F]FDG-2NNC2ON and [^{18}F]FDG-2NNC5ON

In 2019, Yang et al. reported the [^{18}F]FDG-labeled 2-nitroimidazole derivatives [^{18}F]FDG-2NNC2ON ([^{18}F]24a) and [^{18}F]FDG-2NNC5ON ([^{18}F]24b) [18]. Phthalimide potassium salts 18 were coupled with dibromides 19a–b in the presence of K_2CO_3 in MeCN to yield compounds 20a–b, which subsequently underwent substitution reaction with 2-nitroimidazole in the presence of K_2CO_3 in acetonitrile to produce compounds 21a–b, respectively. Compounds 22a–b were synthesized via reactions of 21a–b with $NH_2NH_2{\cdot}H_2O$ in ethanol. The reaction of 22a-b with Boc-aminooxy acetic acid (Boc-Aoa), 1-ethyl-(3-dimethylaminopropyl)carbodiimide hydrochloride (EDCl), 1-hydroxybenzotriazole hydrate (HOBt) and Et_3N generated precursors 23a (2NNC2ON) and 23b (2NNC5ON). Radiolabeling precursors 23a and 23b with [^{18}F]FDG in the presence of HCl in DMSO/H_2O, followed by purification afforded the desired radiotracers [^{18}F]24a and [^{18}F]24b with RCY of 57.6 ± 8.1 and 59.5 ± 9.5%, specific activities of 51.8–106.6 and 53.6–110.1, respectively, and >99% radiochemical purity (Fig. 5). Even though of [^{18}F]24a and [^{18}F]24b had low tumor uptake values, in the PET imaging study, the accumulation of [^{18}F]24a and [^{18}F]24b were observable in OS732 and S180 tumor-bearing mice since 1 h p.i.

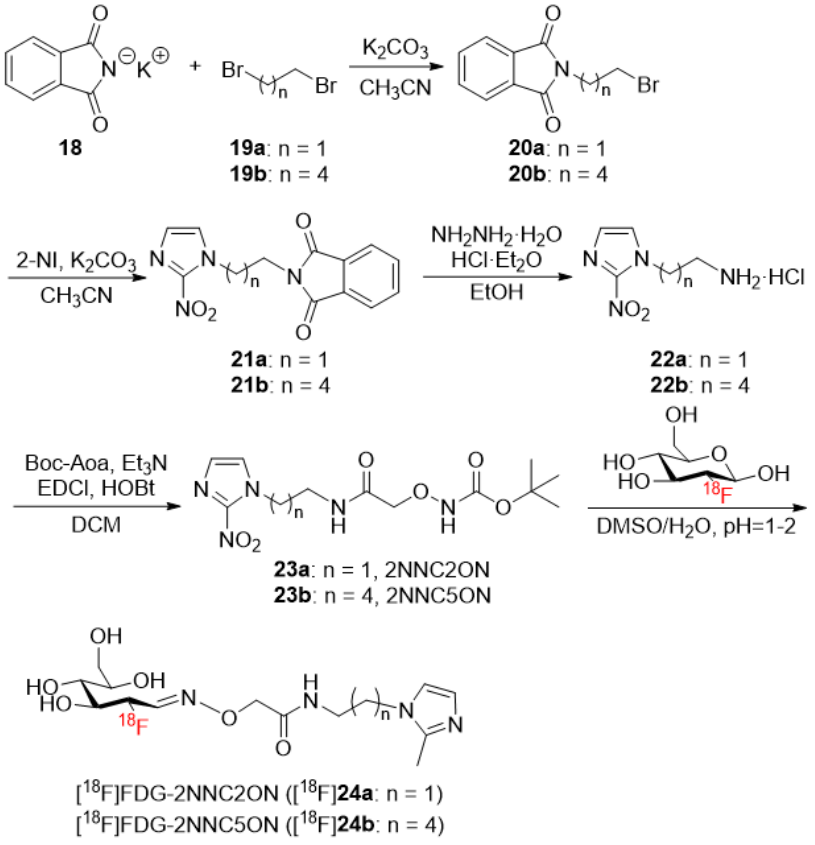

Fig. 5. Synthetic pathways of precursors 2NNC2ON and 2NNC5ON and radiosynthesis of [^{18}F]FDG-2NNC2ON and [^{18}F]FDG-2NNC5ON.

2. ^{18}F-labeled radiotracers containing linkers

1. Synthesis of ^{18}F-labeled nitroimidazole derivatives containing PEG linkers

In 2017, Cao et al. reported several ^{18}F-labeled nitroimidazole derivatives with different polyethylene glycol (PEG) linkers via click reaction [19]. Reactions of PEGs 25a-c with 3-bromo-prop-1-yne 26 in the presence of NaOH produced PEG-modified alkynes 27a–c. Tosylation of 27a-c with TsCl gave precursors 28a-c. Regarding the synthesis of the nitroimidazole precursor 31, the tosylation of compound 29 provided

compound 30, which was then converted to precursor 31 bearing an azide group via a reaction with NaN_3 in DMF. PEG-modified precursor 33a-c was prepared via the substitution reaction of di-tosylated PEG 32a-c with NaN_3 in DMF. Precursor 34 was synthesized from alkyne 26 and compound 29 in the presence of NaOH. PEG compounds 35a-d were di-tosylated by TsCl, then reacted with 2-nitroimidazole to form compounds 36a-d. Precursors 37a-d were prepared via reactions of 36a-d with NaN_3 in DMF. Radiolabeling reaction and click reaction were employed for the synthesis of ten ^{18}F-labeled radiotracers. Radiolabeling of tosylated precursors 28a-c and 33a-c with [^{18}F]fluoride produced compounds [^{18}F]38a-c and [^{18}F]40a-c. Radiofluorinated compounds [^{18}F]38a-c and [^{18}F]40a-c and precursors bearing nitroimidazole (31, 34, 37a-d) were coupled via cycloaddition reactions between azide and alkyne groups to afford the desired radiotracers ([^{18}F]39a–c, [^{18}F]41a–c, and [^{18}F]42a–d) (Fig. 6). The ten radiotracers exhibited tumor uptake values ranging from 1.46 to 2.99 %ID/g at 1 h p.i. when tested in vivo biodistribution studies using EMT-6-tumor bearing BALB/c mice.

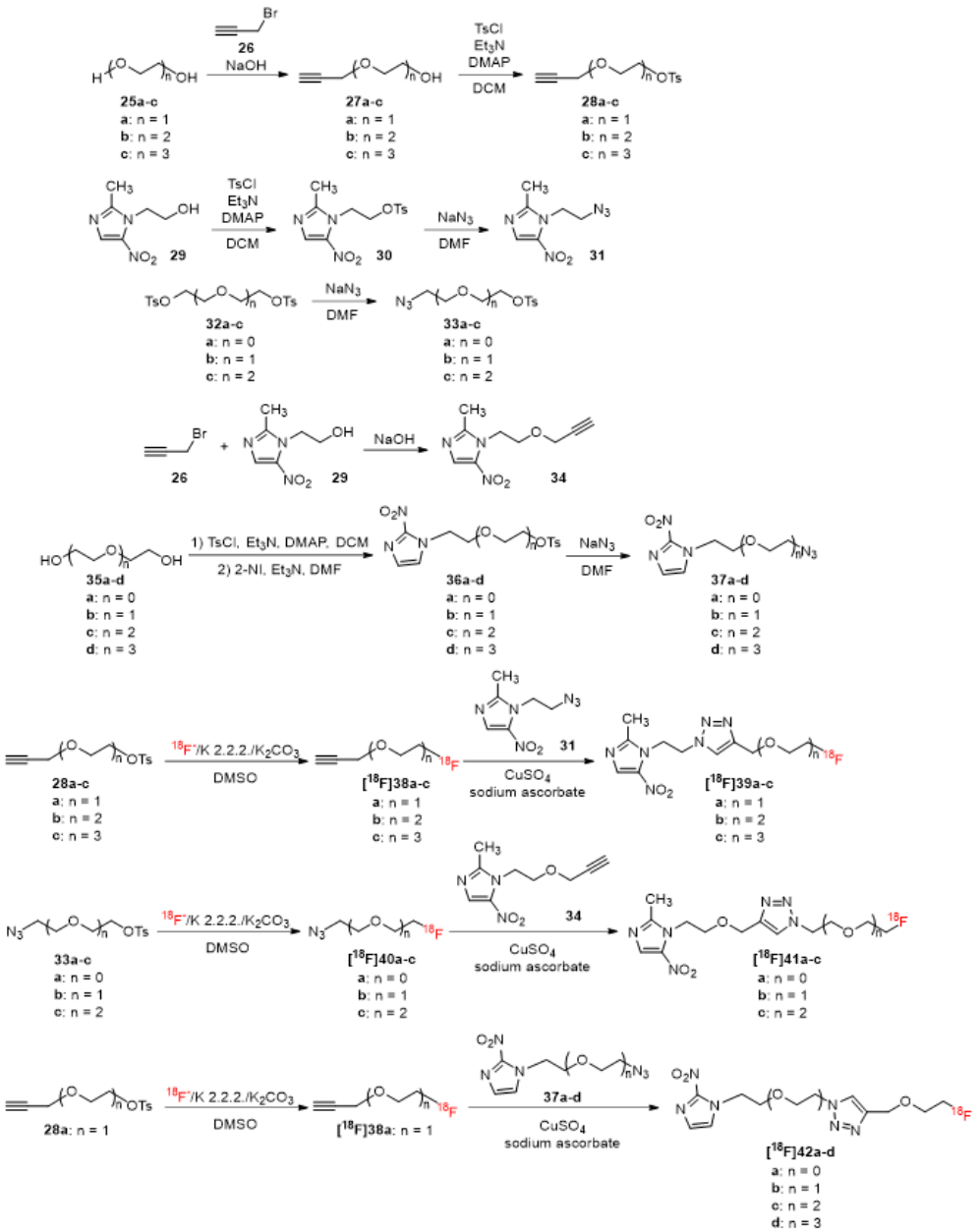

Fig. 6. Synthetic procedures for azides and alkynes precursors and radiosynthesis of ^{18}F-labeled PEG-modified nitroimidazole derivatives via click reaction.

2. Synthesis of ^{18}F-labeled pimonidazole derivatives and nitroimidazole derivatives bearing sulfonyl linkers

In 2021, ^{18}F-labeled pimonidazole derivatives and nitroimidazole derivatives containing sulfonyl as linkers were reported by Wang et al [20]. The ^{18}F-radiofluorination of di-tosylate-PEG1 43 and di-tosylate-PEG2 49 with [^{18}F]TBAF provided two corresponding ^{18}F-radiolabeled compounds, which subsequently underwent substitution of tosylates with amine groups of piperazine 45 to produce compounds [^{18}F]46 and [^{18}F]50. [^{18}F]53 was prepared via substitution reaction of [^{18}F]44 and homopiperazine 52. The ^{18}F-labeled radiotracers ([^{18}F]48, [^{18}F]51, and [^{18}F]54) were synthesized with moderate RCY (22.8–29.0%) via reactions of [^{18}F]46, [^{18}F]50, and [^{18}F]53, respectively, with 1-(2,3-epoxypropyl)-2-nitroimidazole 47 in the presence of K_2CO_3. Nucleophilic substitution of compounds 55 and 59 with [^{18}F]TBAF generated compounds [^{18}F]56 and [^{18}F]60, respectively. Reactions of [^{18}F]56 and [^{18}F]60 with 2-nitroimidazole in borate buffer and DMSO produced [^{18}F]57 and [^{18}F]61 in 58.7% and 53.1% RCY, respectively. [^{18}F]58 was prepared in 66.8% RCY from [^{18}F]56 and 4-nitroimidazole in borate buffer and DMSO (Fig. 7). Six radiotracers were obtained with >95% radiochemical purity. PET imaging studies of radiotracers [^{18}F]48, [^{18}F]51, [^{18}F]54 and [^{18}F]57 in FaDu tumor-bearing mice showed that the ^{18}F-labeled nitroimidazole derivative [^{18}F]57 was the most potential with high tumor uptakes and tumor-to-muscle ratios.

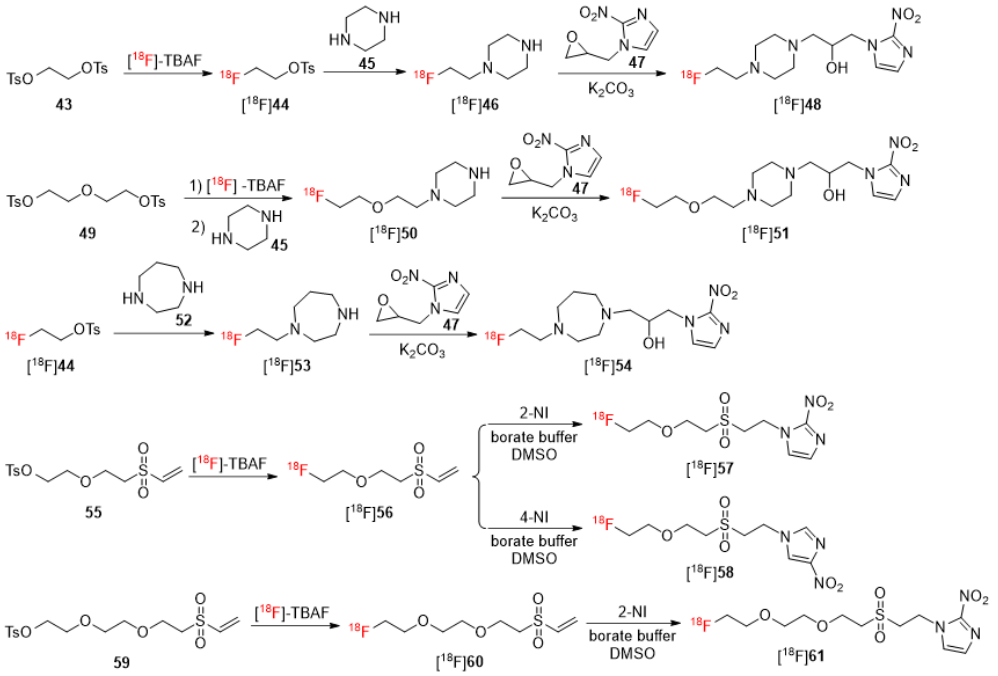

Fig. 7. Synthetic procedures for ^{18}F-labeled pimonidazole derivatives and nitroimidazole derivatives bearing sulfonyl linkers.

3. Synthesis of [^{18}F]FBNA

[^{18}F]FBNA (N-(4-[^{18}F]fluorobenzyl)-2-(2-nitro-1H-imidazol-1-yl)acetamide) is a ^{18}F-labeled derivative of the cytotoxic agent benzonidazole synthesized by Nario et al. in 2022 [21]. The reaction of 2-nitroimidazole and ethyl-2-bromoacetate 63 in the presence of K_2CO_3 in acetonitrile, followed by hydrolysis of the ester group of 64 with NaOH in water/MeOH afforded compound 65 containing 2-nitroimidazole. Precursor [^{18}F]FBA ([^{18}F]66) was synthesized via the radiofluorination of 4-cyano-*N,N,N*-trimethylanilinium trifluoro-methanesulfonate with [^{18}F]fluoride/K_{222} in acetonitrile [22]. An acylation reaction of the activated carboxylic group of 65 with [^{18}F]FBA in the presence of EDC and DIPEA in THF produced the desired radiotracers ([^{18}F]67) with moderate RCY, high radiochemical purity and molar activity of >40 GBq/μmol (Fig. 8). When tested in vitro in the AGS and MKN45 cancer cell lines, [^{18}F]FBNA demonstrated selective uptake in both cell lines under hypoxic conditions rather than normoxic conditions.

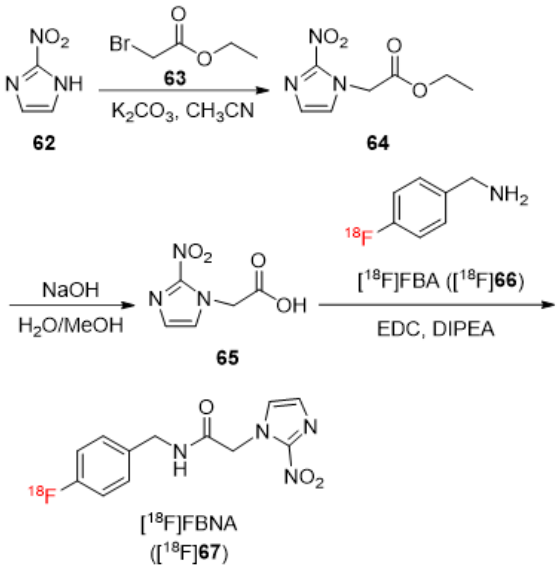

Fig. 8. Synthetic of ^{18}F-labeled radiotracer [^{18}F]FBNA.

3. ^{18}F-labeled radiotracers containing B–^{18}F or Al–^{18}F bond

1. Synthesis of ^{18}F - AmBF$_3$ - Bu - 2NI

In 2017, ^{18}F-nitroimidazole derivative containing zwitterion AmBF$_3$ - Bu - 2NI ([^{18}F]75) was designed and synthesized by Nunes et al. [23]. 2-Nitroimidazole was coupled with 1,4 - dibromobutane 69 in the presence of K_2CO_3 in DMF to produce compound 70, which then reacted with dimethylamine in an EtOH/THF mixture to generate compound 72. The reaction of 72 with iodomethylboronic acid pinacol ester 73, followed by a reaction with KHF_2 in the presence of HCl and H_2O in DMF afforded the product AmBF$_3$ - Bu - 2NI (74). Radiofluorination of AmBF$_3$ - Bu - 2NI via ^{18}F-^{19}F isotope exchange reaction produced desired radiotracer ([^{18}F]75) with 14.8 ± 0.4% RCY, 24.5 ± 5.2 GBq/μmol specific activity and good radiochemical purity (>99%) (Fig. 9). In vivo biodistribution study in HT-29 tumor-bearing mice showed that AmBF$_3$ - Bu - 2NI had low tumor uptake and tumor-to-background ratios. Hence, the accumulation of [^{18}F]75 was only detectable in PET images of HT-29 tumor-bearing mice after 3 h p.i.

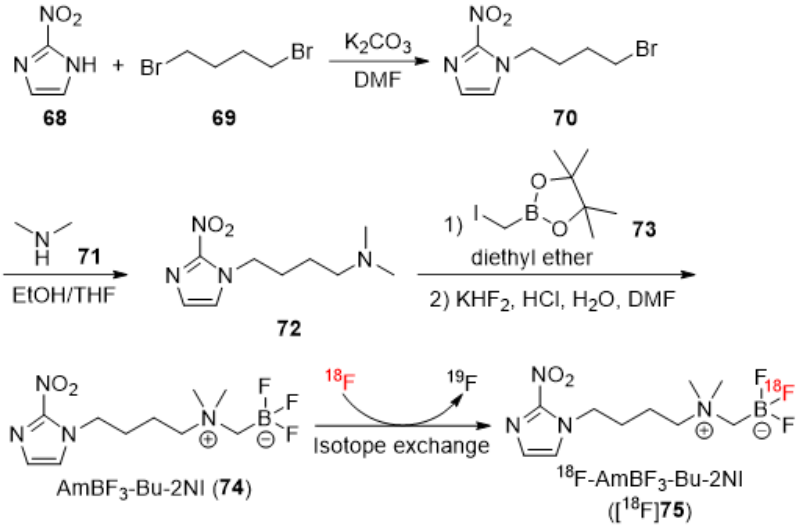

Fig. 9. Synthesis and radiofluorination precursor AmBF$_3$ - Bu - 2NI.

2. Synthesis of Al^{18}F-NOTA-NI

In 2021, radiotracer Al^{18}F-NOTA-NI ([^{18}F]85) was prepared from precursor NOTA-NI (2-[4-(carboxymethyl)-7-[2-(2-(2-nitro-1H-imidazol-1-yl)acetamido)ethyl]-1,4,7-triazanonan-1-yl]acetic acid) via radiofluorination with aluminum-fluoride (Al^{18}F) by Lu et al. [24]. The compound 2-nitroimidazole (76) reacted with *tert*-butyl 2-bromoacetate 77 in the presence of K_2CO_3 in acetonitrile to give compound 78. Hydrolysis of 78 by TFA in DCM produced compound 79, which then reacted with 2-bromoethanamine hydrobromide 80, HATU (2-(7-azabenzotriazol-1-yl)-N,N,N′,N′-tetramethyluronium hexafluorophosphate) and DIEA (N,N-diisopropylethylamine) in DCM and DMF to generate compound 81. Compound 83 was prepared via the reaction of triazacyclononane 82 and *tert*-butyl bromoacetate in $CHCl_3$. Substitution reaction of 83 with 81 in the presence of K_2CO_3 in acetonitrile, followed by the deprotection of an ester group with TFA afforded the precursor NOTA-NI. The radiofluorination of precursor NOTA-NI with $AlCl_3$ and ^{18}F solution at pH 3.5 generated radiotracer [^{18}F]85 with 52.6 ± 3.7% RCY, 50 GBq/μmol specific activity, and >95% radiochemical purity (Fig. 10). In ECA109-tumor bearing mice, [^{18}F]60 was rapidly excreted due to high hydrophilicity, therefore, its initial tumor uptake was lower compared to [^{18}F]FMISO. However, [^{18}F]85 exhibited a higher tumor-to-muscle contrast than [^{18}F]FMISO.

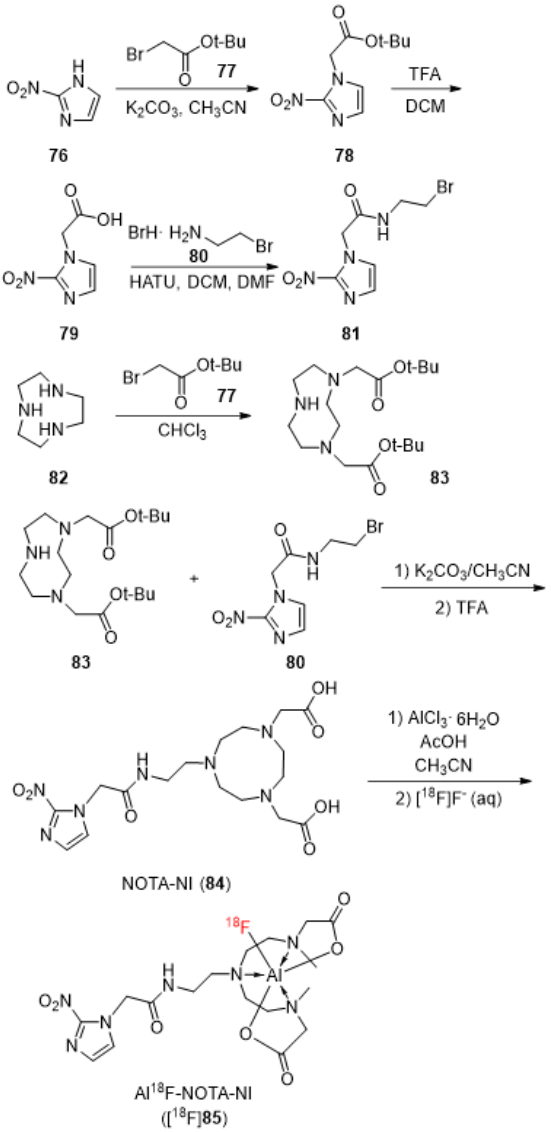

Fig. 10. Synthetic route to precursor NOTA-NI and radiosynthesis of radiotracer Al^{18}F-NOTA-NI

Conclusion

Hypoxia is frequently found in most solid tumors and can affect cancer progression, as well as increases the risk of negative response to cancer therapies. Thus, design and synthesis of suitable radiopharmaceuticals for the effective and precise detection of tumor hypoxia is crucial to cancer prognosis and treatments. Since the first generation of hypoxia-targeting radiopharmaceuticals was developed, extensively investigation has been conducted on ^{18}F-labeled nitroimidazole derivatives. In recent years, numerous compounds have been synthesized and radiofluorinated to produce a variety of ^{18}F-labeled radiotracers with improved pharmacokinetics and selectivity for hypoxia. It is noteworthy that the development of ^{18}F-labeled radiotracers containing nitroimidazole shows great potential due to the advantageous chemical and physical properties of fluorine-18. This review presents a detailed overview of the recent synthetic routes and radiolabeling of ^{18}F-labeled-nitroimidazole radiotracers for the detection of tumor hypoxia.

REFERENCES

1. Weissleder R, Mahmood U. Molecular imaging. Radiology. 2001;219(2):316–33.
2. Pysz MA, Gambhir SS, Willmann JK. Molecular imaging: current status and emerging strategies. Clin Radiol. 2010;65(7):500-16.
3. Ollinger JM, Fessler JA. Positron Emission Tomography. IEEE Signal Process Magazine. 1997;14(1):43–55.
4. Weber WA, Czernin J, Anderson CJ, Badawi RD, Barthel H, Bengel F, et al. The Future of Nuclear Medicine, Molecular Imaging, and Theranostics. J Nucl Med. 2020;61(Suppl 2):263S-272S.
5. Lu FM, Yuan Z. PET/SPECT molecular imaging in clinical neuroscience: recent advances in the investigation of CNS diseases. Quant Imaging Med Surg. 2015;5(3):433-47.
6. Unterrainer M, Eze C, Ilhan H, Marschner S, Roengvoraphoj O, Schmidt-Hegemann NS, et al. Recent advances of PET imaging in clinical radiation oncology. Radiat Oncol. 2020;15(1):88.
7. Parker CC, Lapi SE. Positron Emission Tomography Imaging of Macrophages in Cancer. Cancers. 2021; 13(8):1921.
8. Ma Y, Wang Q, Dong Q, Zhan L, Zhang J. How to differentiate pseudoprogression from true progression in cancer patients treated with immunotherapy. Am J Cancer Res. 2019;9(8):1546-53.
9. Li Y, Zhao L, Li XF. Hypoxia and the Tumor Microenvironment. Technol Cancer Res Treat. 2021;20:15330338211036304.
10. Nejad AE, Najafgholian S, Rostami A, Sistani A, Shojaeifar S, Esparvarinha M, et al. The role of hypoxia in the tumor microenvironment and development of cancer stem cell: a novel approach to developing treatment. Cancer Cell Int. 2021(1);21:62.
11. Mittal S, Mallia MB. Molecular imaging of tumor hypoxia: Evolution of nitroimidazole radiopharmaceuticals and insights for future development. Bioorg Chem. 2023;139:106687.
12. Jacobson O, Kiesewetter DO, Chen X. Fluorine-18 radiochemistry, labeling strategies and synthetic routes. Bioconjug Chem. 2015;26(1):1-18.
13. Wanek T, Kreis K, Križková P, Schweifer A, Denk C, Stanek J, et al. Synthesis and preclinical characterization of 1-(6'-deoxy-6'-[^{18}F]fluoro-β-d-allofuranosyl)-2-nitroimidazole (β-6'-[^{18}F]FAZAL) as a positron emission tomography radiotracer to assess tumor hypoxia. Bioorg Med Chem. 2016;24(21):5326-39.
14. Schweifer A, Hammerschmidt F. Preparation of Nucleosides Derived from 2-Nitroimidazole and d-Arabinose, d-Ribose, and d-Galactose by the Vorbrüggen Method and Their Conversion to Potential Precursors for Tracers to Image Hypoxia. J Org Chem. 2011;76(20):8159–67.
15. Schweifer A, Maier F, Ehrlichmann W, Lamparter D, Kneilling M, Pichler BJ, et al. [^{18}F]Fluoro-Azomycin-2´-Deoxy-β-D-Ribofuranoside – A New Imaging Agent for Tumor Hypoxia in Comparison with [^{18}F]FAZA. Nucl Med Biol 2016;43(12):759–69.
16. Maier FC, Schweifer A, Damaraju VL, Cass CE, Bowden GD, et al. 2-Nitroimidazole-Furanoside Derivatives for Hypoxia Imaging-Investigation of Nucleoside Transporter Interaction, ^{18}F-Labeling and Preclinical PET Imaging. Pharmaceuticals 2019:12(1):31.
17. Kumar P, Ohkura K, Beiki D, Wiebe LI, Seki KI. Synthesis of 1-β-D-(5-Deoxy-5-Iodoarabinofuranosyl)-2-Nitroimidazole (β-IAZA): A Novel Marker of Tissue Hypoxia. Chem Pharm Bull. 2003;51(4):399–403.
18. Yang X, Wang F, Zhu H, Yang Z, Chu T. Synthesis and Bioevaluation of Novel [^{18}F]FDG-Conjugated 2-Nitroimidazole Derivatives for Tumor Hypoxia Imaging. Mol Pharm. 2019;16(5):2118–28.

19. Cao J, Liu Y, Zhang L, Du F, Ci Y, Zhang Y, et al. Synthesis of Novel PEG-Modified Nitroimidazole Derivatives via "Hot-Click" Reaction and Their Biological Evaluation as Potential PET Imaging Agent for Tumors. J Radioanal Nucl Chem. 2017;312(2):263–76.
20. Wang L, Wang H, Shen K, Park H, Zhang T, Wu X, et al. Development of Novel ^{18}F-PET Agents for Tumor Hypoxia Imaging. J Med Chem. 2021;64(9):5593–602.
21. Nario AP, Woodfield J, Dos Santos SN, Bergman C, Wuest M, Araújo YB, et al. Synthesis of a 2-nitroimidazole derivative N-(4-[^{18}F]fluorobenzyl)-2-(2-nitro-1H-imidazol-1-yl)-acetamide ([^{18}F]FBNA) as PET radiotracer for imaging tumor hypoxia. EJNMMI Radiopharm Chem. 2022;7(1):13.
22. Way J, Wuest F. Fully automated synthesis of 4-[^{18}F]fluorobenzylamine based on borohydride/$NiCl_2$ reduction. Nucl Med Biol. 2013;40(3):430-6.
23. Nunes PSG, Zhang Z, Kuo HT, Zhang C, Rousseau J, Rousseau E, et al. Synthesis and Evaluation of an ^{18}F-Labeled Trifluoroborate Derivative of 2-Nitroimidazole for Imaging Tumor Hypoxia with Positron Emission Tomography. J Label Compd Radiopharm. 2018;61(4):370–9.
24. Lu J, Zhang C, Yang X, Yao XJ, Zhang Q, Sun XC. Synthesis and Preliminary Evaluation of a Novel ^{18}F-Labeled 2-Nitroimidazole Derivative for Hypoxia Imaging. Front Oncol. 2021;10:1–9.